Statistical mechanics of combinatorial optimization problems with site disorder

David S. Dean,[1] David Lancaster,[2] and Satya N. Majumdar[3]
[1]*Laboratoire de Physique Théorique, UMR CNRS 5152, IRSAMC, Université Paul Sabatier, 118 route de Narbonne, 31062 Toulouse Cedex 04, France*
[2]*Harrow School of Computer Science, University of Westminster, Harrow, HA1 3TP, United Kingdom*
[3]*Laboratoire de Physique Théorique et Modèles Statistiques, UMR 8626, Université Paris Sud, Bât 100, 91045 Orsay Cedex, France*
(Received 19 April 2005; published 22 August 2005)

We study the statistical mechanics of a class of problems whose phase space is the set of permutations of an ensemble of quenched random positions. Specific examples analyzed are the finite-temperature traveling salesman problem on several different domains and various problems in one dimension such as the so-called descent problem. We first motivate our method by analyzing these problems using the annealed approximation. Then in the limit of a large number of points we develop a formalism to carry out the quenched calculation. This formalism does not require the replica method, and its predictions are found to agree with Monte Carlo simulations. In addition our method reproduces an exact mathematical result for the maximum traveling salesman problem in two dimensions and suggests its generalization to higher dimensions. The general approach may provide an alternative method to study certain systems with quenched disorder.

DOI: 10.1103/PhysRevE.72.026125 PACS number(s): 89.75.−k, 05.20.−y, 46.15.Cc

I. INTRODUCTION

The statistical mechanical approach to the study of optimization problems has led to progress in a number of ways. The approach is based on identifying the cost function, which needs to be minimized, with the energy of a physical system whose phase space is equivalent to the free adjustable parameters in the optimization problem. The zero-temperature energy of the resulting physical system thus corresponds to the optimal solution. This formulation can be exploited in two ways. First, physically motivated minimization techniques such as simulated annealing can be applied to optimization problems [1], often leading to near-optimal solutions. Second, the statistical mechanical approach can also be used to carry out computations of average or typical values of optimal solutions, where the nonadjustable parameters (describing the realization of the instance) in the system are taken to be quenched random variables [2]. The replica and cavity methods, which are much used in the theory of spin glasses, have been successfully exploited to study statistical properties in wide range of optimization problems [2–5]. Often optimization problems have a phase space which is equivalent to permutations or partitions of the integers and these problems are referred to as combinatorial optimization problems. One of the most famous of these combinatorial problems is the traveling salesman problem (TSP). Here the problem is to find the minimal circuit length to visit N cities or points where the distance between the points i and j is given by d_{ij}. The order in which the cites are visited is encoded in a permutation $\sigma \in \Sigma_N$ where Σ_N is the group of permutations of N objects. For a given permutation,

$$D(\sigma) = \sum_i d_{\sigma_i,\sigma_{i+1}} \tag{1}$$

is the corresponding total distance traveled. When the d_{ij}'s are chosen from some quenched distribution the problem is referred to as the stochastic TSP. The most natural form of the TSP is the Euclidean TSP [6] where the cities are points $\mathbf{r}_1, \mathbf{r}_2, \ldots, \mathbf{r}_N$, in some connected domain $\mathcal{D}$ in $\mathbb{R}^d$ and each point is independently distributed from the others with the same probability density function $p_q(\mathbf{r})$. The distance between the points i and j is simply the Euclidean distance on $\mathbb{R}^d$ given by $d_{ij} = |\mathbf{r}_i - \mathbf{r}_j|$. It was shown [6] that for $N \to \infty$ the minimal path D_M behaves as

$$\frac{D_M}{N^{1-1/d}} \to \beta(d) \int_{\mathcal{D}} d^d r [p_q(\mathbf{r})]^{1-1/d}, \tag{2}$$

with probability 1. Here $\beta(d)$ is a constant depending on the dimension of the space d but independent of p_q. The stochastic TSP has also been studied under the *random link* hypothesis where the d_{ij} are all uncorrelated (up to any symmetry requirement). Clearly in this random link version the triangle inequality is not respected. This version has been intensively studied [7–11], and its analysis is greatly simplified by the lack of correlation between the d_{ij} which makes the taking of the disorder average quite straightforward. A, somewhat perverse, variant of the TSP is one where one asks for the maximal tour; this is called the maximum TSP [12] and is, for obvious reasons, sometimes referred to as the taxicab rip-off. In the statistical mechanical formulation, if one looks for the maximal tour, one keeps the same cost function but changes the sign of the temperature.

In the class of problems we shall study in this paper, N points $\{\mathbf{r}_1, \mathbf{r}_2 \ldots, \mathbf{r}_N\}$ are chosen independently in some domain $\mathcal{D} \in \mathbb{R}^d$ with probability density $p_q(\mathbf{r})$. Again the dynamical phase space for the problem is taken to be all permutations of the order of these points, $\sigma \in \Sigma_N$. The Hamiltonian for the system is defined to be

$$H(\sigma) = \sum_{i=1}^{N} V(\mathbf{r}_{\sigma_i} - \mathbf{r}_{\sigma_{i-1}}). \tag{3}$$

Cyclic boundary conditions $\mathbf{r}_0 = \mathbf{r}_N$ are imposed. In this context the Euclidean TSP corresponds to the zero-temperature limit of the case where $V(\mathbf{r}) = |\mathbf{r}|$.

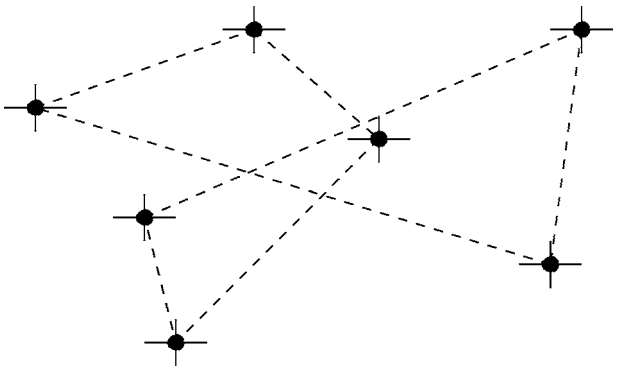

FIG. 1. Ring polymer on a two-dimensional substrate where each monomer (solid circles) is attached to an impurity (crosses).

A physical realization of the system is one where the $\mathbf{r}_i$ are impurities where the monomers of a polymer loop are pinned and only one monomer can be pinned per impurity. The potential V represents effective interaction between neighboring monomers on the chain. For instance, $V(\mathbf{r}) = \lambda r^2/2$ corresponds to the Rouse model of a polymer chain [13]. For instance, in Fig. 1 we represent the system of a polymer on a two-dimensional substrate where the monomers, shown as solid circles, attach themselves to pinning sites (shown as crosses).

The canonical partition function for these problems is given by the following sum over all permutations:

$$Z_N = \frac{1}{N!} \sum_{\sigma \in \Sigma_N} \exp[-\beta H(\sigma)]. \tag{4}$$

Since the number of permutations grows as $N!$, the entropy is nonextensive and behaves as $N \ln N$, but here we insert a factor of $1/N!$ to absorb it.

To compute the average energy per site it is necessary to work out the quenched free energy of the system:

$$F_N = -\frac{1}{\beta} \overline{\ln(Z_N)}, \tag{5}$$

where the overbar denotes averaging with respect to the quenched joint probability density function of the random sites $\mathbf{r}_i$. The energy per site is then evaluated as

$$\epsilon = \frac{1}{N} \frac{\partial}{\partial \beta} \beta F_N. \tag{6}$$

Our method will be shown to be exact in the limit of large N while keeping the domain $\mathcal{D}$ fixed. However, this large-N scaling is not the one needed to obtain the quantity $\beta(d)$ in Eq. (2). When the probability density $p_q(\mathbf{r})$ is flat and $V(\mathbf{r})$ is an attractive potential, as is the case for the ordinary TSP, the minimal energy configuration is one where links are always of the order of the minimal separation between points—that is to say, $O(\rho^{-1/d})$ where ρ is the density of points—and thus the ground energy per site is of the order

$$\epsilon_{GS} \approx V(\rho^{-1/d}). \tag{7}$$

If one uses the TSP potential $V(\mathbf{r}) = |\mathbf{r}|$ in the above, one recovers the scaling of Eq. (2). In these attractive cases the ground-state energy per site is zero in the thermodynamic limit and in order to extract an extensive result the energy of the system must be scaled appropriately with N [3]. If the potential V is repulsive, as in the maximum TSP, then links will be typically of the domain size $\mathcal{D}$ and if this domain size is $O(1)$ (in the sense that it does not scale with N), then the ground-state energy per site will be $O(1)$ without the need for any special scaling.

We emphasize that our method is exact in any dimension; however, many of the examples we give will be in one dimension, where many explicit results can be obtained. In one dimension we remark that any attractive choice of the potential V corresponds to a choice of cost function for the computational problem of sorting random data elements into increasing order. The performance of local physical Monte Carlo algorithms has been analyzed in problems with these cost functions [16], demonstrating the pitfalls in using such algorithms to search for the optimum. Indeed tree-based sorting algorithms are much more efficient [15].

The main potential we shall investigate is

$$V(\mathbf{r}) = |\mathbf{r}|, \tag{8}$$

and, as mentioned previously, this potential is of particular interest as it arises naturally in the Euclidean TSP as its ground state at positive temperature is the shortest circuit visiting each of the points once and only once. We will discuss this problem in detail in both one and two dimensions on several domains with different topologies. Some of these domains are not simply connected, and besides the average energy observable, which is our main focus, we show how to compute the statistics of the winding number of the path around the domain. Of course the solution to the one-dimensional TSP is obvious; one starts with the leftmost point and works along to the rightmost, giving an average ground state energy per site of $\epsilon_{GS}=0$. Using the scaling of this paper the ground-state energy of the ordinary TSP per site is $\epsilon_{GS}=0$ in all dimensions, as can be seen from Eq. (2). At negative temperature (or where the sign of V is inverted) the corresponding ground state corresponds to the solution of the maximum TSP where one requires the maximal distance taken to complete a circuit visiting all the points once and only once. The solution here is not quite so obvious but we shall see that $\epsilon_{GS}=1/2$ is the average ground-state energy per site. For a uniform distribution of points the interested reader may verify that this average value of ϵ_{GS} may be achieved by a greedy algorithm, which starts at the leftmost point, goes to the rightmost point, returns to the next leftmost point, and so on. We emphasize, however, that the main point of this paper is to solve the finite-temperature statistical mechanics of these models at all temperatures.

We shall also consider the descent problem [14] as a fully soluble system in which all our equations can be resolved analytically. This is a one-dimensional system described by the potential

$$V(x) = \theta(-x) \tag{9}$$

for $x \in [0,1]$. In fact the original formulation of the descent model is equivalent to one where x_i are chosen to deterministically as $x_i = i/N$. However, because of the scale-free na-

ture of the potential V, all models with an arbitrary continuous distribution of the x_i are in fact equivalent. The energy of the permutation is thus the number of points where x_{σ_i} is greater than the point $x_{\sigma_{i+1}}$, the point which follows it on the polymer ring. The ground state of the system is simply the permutation in which the x_{σ_i} appear in increasing order and has corresponding energy per site $\epsilon_{GS}=0$.

To further test the validity of our method, we have considered harmonic potentials $V(\mathbf{r})=|\mathbf{r}|^2$ in various dimensions. In one dimension with domain $x_i \in [0,1]$, we have also studied the potential $V(x)=-\ln(|x|)$ at positive temperatures (where the model is defined).

In all cases studied the analytic predictions were confirmed by Monte Carlo simulations and in some cases by extrapolating the results of exact enumeration for systems of small size. In addition the behavior of ϵ_{GS} for repulsive potentials V in one dimension is analyzed via a zero-temperature analysis and the results are discussed in terms of the corresponding optimal paths. We also examine the maximum TSP in higher dimensions and show that we recover an exact mathematical result for the average length of the optimal path in two dimensions. We are able to use our method to predict the corresponding optimal path length in higher dimensions. A fascinating aspect of this analysis is that, in addition to providing the average optimal path length, the saddle point equations we derive in the thermodynamic limit seem to suggest the heuristic one should use to search for the optimal path.

As this paper is rather long and also contains lots of examples, we conclude this Introduction with a description of the following sections.

In Sec. II we study the annealed approximation for a general interaction potential. The finite-temperature behavior of several models is then discussed, and the physical mechanism leading to the difference between the annealed and quenched calculations is highlighted. We find that the annealed approximation is exact for the descent model and explain why.

In Sec. III the general formalism for the quenched calculation is developed—this is the core and key idea of the paper. Various examples are analyzed, for general temperatures, and compared with Monte Carlo simulations.

In Sec. IV we concentrate on the zero-temperature limit of the quenched calculations and thus make contact with the corresponding optimization problems. Most of this analysis is for one-dimensional problems, where analytic results can be obtained and some classification of the optimal path is possible in terms of the convexity or concavity of the interaction potential V. The maximal TSP is analyzed in general dimensions and a conjecture for the length of the maximal path put forward.

In Sec. V we present our conclusions and perspectives for further studies.

A brief description of our method has appeared in Ref. [17] and a comment on the technique can be found at http://jc-cond-mat.bel-labs.com.

II. ANNEALED APPROXIMATION

A. General formalism

Here we shall analyze the statistical mechanics of this general class of problems in the annealed approximation which amounts to setting

$$F_N \approx F_N^{ann} = -\frac{1}{\beta}\ln(\bar{Z}_N). \tag{10}$$

This approximation is in general doomed to failure for the following reason. In the annealed approximation the quenched variables are no longer quenched and will evolve dynamically in order to decrease the free energy of the system. The configuration of variables which dominates the thermodynamics will generically be atypical of the initial quenched distribution and will usually be of measure zero. For instance, if we consider the one-dimensional TSP at negative temperature, it is clear that the maximal circuit, averaging over all permutations and positions x_i, will be one where half the x_i are at the point $x=0$ and the other half at $x=1$. This will allow a ground-state energy of $\epsilon_{GS}=1$ from applying the greedy algorithm mentioned in the Introduction. However, this configuration is of measure zero if the quenched distribution is uniform on $[0,1]$. Despite this deficiency, the formalism below will have an important bearing on our subsequent development of the quenched calculation and indeed its physical interpretation.

The partition function is averaged over all $\mathbf{r}_i$, $i=1,\ldots,N$, with periodic boundary conditions—i.e., $\mathbf{r}_0=\mathbf{r}_N$. Upon this averaging all permutations become equivalent and we obtain

$$\overline{Z_N} = \int \prod_{i=1}^{N} d^d r_i \exp\left(-\beta \sum_{i=1}^{N} V(\mathbf{r}_i - \mathbf{r}_{i-1})\right). \tag{11}$$

The above averaged partition function can be evaluated using standard transfer operator techniques,

$$\overline{Z_N} = \mathrm{Tr}\, T^N = \int d^d r T^N(\mathbf{r},\mathbf{r}), \tag{12}$$

where T is the operator:

$$T(\mathbf{r},\mathbf{r}') = \exp[-\beta V(\mathbf{r}-\mathbf{r}')]. \tag{13}$$

In the limit of large N, taking the size of the domain to be normalized to unity, we find

$$\overline{Z_N} = \lambda_a^N, \tag{14}$$

where λ_a is the largest eigenvalue of the operator T (we use the subscript a to indicate a quantity evaluated in the annealed approximation). The corresponding right and left eigenfunctions $f_{R,L}^{(a)}$ of T obey

$$f_R^{(a)}(\mathbf{r}) = \lambda_a^{-1} \int d^d r' \exp[-\beta V(\mathbf{r}-\mathbf{r}')] f_R^{(a)}(\mathbf{r}'), \tag{15}$$

$$f_L^{(a)}(\mathbf{r}) = \lambda_a^{-1} \int d^d r' \exp[-\beta V(\mathbf{r}'-\mathbf{r})] f_L^{(a)}(\mathbf{r}'). \tag{16}$$

These eigenfunctions are identical for a symmetric potential, and we chose the eigenfunctions to be normalized.

In this eigensystem, λ_a can have several solutions but that with the maximum value of λ_a dominates the partition function at large N. Moreover, the eigenfunctions $f_{R,L}^{(a)}$ corresponding to the largest eigenvalue must be positive by the Perron-Frobenius theorem. The annealed approximation for the energy per site is consequently obtained as

$$\epsilon_a = -\frac{\partial \ln(\lambda_a)}{\partial \beta}. \tag{17}$$

The annealed density of points $\mathbf{r}_i$ on the path at the point $\mathbf{r}$ is given by

$$p_a(\mathbf{r}) = \frac{1}{N}\left\langle \sum_{j=1}^{N} \delta(\mathbf{r}-\mathbf{r}_j) \right\rangle, \tag{18}$$

where the angular brackets indicate the Gibbs ensemble average over the annealed points. From the periodic boundary conditions, all points are equivalent and we have

$$p_a(\mathbf{r}) = \langle \delta(\mathbf{r}-\mathbf{r}_1)\rangle = \frac{T^N(\mathbf{r},\mathbf{r})}{\bar{Z}_N} = f_R^{(a)}(\mathbf{r}) f_L^{(a)}(\mathbf{r}), \tag{19}$$

where again we have taken the thermodynamic limit.

In this annealed approximation the probability density of the points is thus given by Eq. (19). In general we will find that

$$p_a(\mathbf{r}) \neq p_q(\mathbf{r}) \tag{20}$$

as the variables $\mathbf{r}_i$ evolve dynamically.

A general expression for the energy at high temperature can be obtained by expanding the averaged partition function for small β. The first two terms of this expansion are

$$\epsilon_a = \int d^d r\, d^d r'\, V(\mathbf{r}-\mathbf{r}') + \beta\left[3\left(\int d^d r\, d^d r'\, V(\mathbf{r}-\mathbf{r}') \right)^2 - 2\int d^d r\, d^d r'\, d^d r''\, V(\mathbf{r}-\mathbf{r}')V(\mathbf{r}'-\mathbf{r}'') - \int d^d r'\, d^d r\, V^2(\mathbf{r}-\mathbf{r}') \right]. \tag{21}$$

A slightly more involved calculation for the quenched case yields the differing expansion

$$\epsilon = \int d^d r\, d^d r'\, V(\mathbf{r}-\mathbf{r}') + \beta\left[2\int d^d r\, d^d r'\, d^d r''\, V(\mathbf{r}-\mathbf{r}')V(\mathbf{r}'-\mathbf{r}'') - \int d^d r\, d^d r'\, V^2(\mathbf{r}-\mathbf{r}') - \left(\int d^d r\, d^d r'\, V(\mathbf{r}-\mathbf{r}') \right)^2 \right]. \tag{22}$$

Thus, in general, there will be a difference between the annealed approximation and quenched result at any finite temperature. We will later check our method for the quenched case by seeing that it reproduces the second form, Eq. (22).

B. Descent model

We start by considering the annealed approximation for the descent model. This model is one dimensional, and throughout this paper we will write $\mathbf{r}=x$ to emphasize when a problem is one dimensional. Differentiating Eq. (16) with respect to x yields

$$\frac{df_R^a}{dx} = \lambda_a^{-1} f_R^a [1-\exp(-\beta)]. \tag{23}$$

This has the solution

$$f_R^a = C\exp(\kappa x), \tag{24}$$

where $\kappa=\lambda_a^{-1}[1-\exp(-\beta)]$ and C is a constant of normalization. This solution is then substituted into the original integral equation to yield $\lambda_a=[1-\exp(-\beta)]/\beta$. Then Eq. (17) gives the annealed energy to be

$$\epsilon_a = \frac{1}{\beta} - \frac{1}{\exp(\beta)-1}. \tag{25}$$

The result, Eq. (25), is in fact identical to that obtained from the exact solution to the descent problem, obtained via more lengthy combinatorial methods [14]. The annealed approximation thus leads to the exact energy per site for this problem. This exactness is straightforward to understand. In this problem there is no length scale in the potential V and only the order of the points determines the energy; clearly, one would obtain the same energy from any continuous distribution of points selected independently with density $p_q(x)$ on $[0,1]$. We note that the solution for the other (left) eigenvector f_L^a is

$$f_L^a = C'\exp(-\kappa x), \tag{26}$$

and we obtain $p_a(x)=1=p_q(x)$; thus, the annealed distribution agrees with the quenched one. This is an autoconsistency of the annealed approximation which leads to it being exact.

C. One-dimensional TSP

In this section we restrict ourselves to one dimension and consider the unit interval with $x\in[0,1]$. We note that the potential V is symmetric and thus may write $f_R^{(a)}=f_L^{(a)}=f^{(a)}$.

We proceed by differentiating Eq. (16) twice to obtain

$$\frac{d^2 f^{(a)}}{dx^2} - \beta^2 f^{(a)} + 2\frac{\beta}{\lambda_a} f^{(a)} = 0, \tag{27}$$

which has the solution

$$f^{(a)} = C[\exp(\omega x) + A\exp(-\omega x)], \tag{28}$$

with

$$\lambda_a^{-1} = \frac{\beta^2-\omega^2}{2\beta}. \tag{29}$$

Now, λ_a must be positive, so we have

$$\omega^2 < \beta^2 \quad \text{for } \beta > 0, \tag{30}$$

$$\omega^2 > \beta^2 \quad \text{for } \beta < 0. \tag{31}$$

Substituting the solution, Eq. (28), back into Eq. (16) we find the condition

$$\exp(2\omega) = \left(\frac{\beta-\omega}{\beta+\omega}\right)^2. \tag{32}$$

We note that a solution of Eq. (32) is $\omega=0$. However, the corresponding solution for $f^{(a)}$ would be of the form $f^{(a)}(x) = Ax+B$. From above one must also have that $df^{(a)}/dx$ is continuous and the clear symmetry $f^{(a)}(x)=f^{(a)}(1-x)$ means that $A=0$ in this solution. One can verify that $f^{(a)}(x)=B$ is not a solution. Hence the solution must have $\omega \neq 0$. For $\beta>0$ one finds that $\omega=i\beta z$ where z is the smallest positive solution of

$$z = \cot(\beta z/2) \tag{33}$$

and shows no discontinuities as β varies. The annealed energy per site is then given by

$$\epsilon_a = \frac{1}{\beta} - \frac{z^2}{1+\frac{1}{2}\beta(1+z^2)}. \tag{34}$$

For $\beta<0$ we find that $\omega=\beta z$ where z is the root of

$$z = \coth(-\beta z/2) \tag{35}$$

and here the annealed energy per site is

$$\epsilon_a = \frac{1}{\beta} + \frac{z^2}{1+\frac{1}{2}\beta(1-z^2)}. \tag{36}$$

In both cases, as $\beta \to 0$ we find that

$$\epsilon_a(0) = \frac{1}{3}, \tag{37}$$

which agrees with the exact high-temperature result, Eq. (21).

In the positive-temperature case the smallest positive solution z^* to Eq. (33) is such that $z^* \in (0, \pi/\beta)$ and thus $z^* \to 0$ as $\beta \to \infty$ and thus $\epsilon_a \approx 1/\beta \to 0$; this clearly agrees with the limiting behavior of the corresponding quenched case. In the case of negative temperature we find that the solution of Eq. (33) behaves as $z^* \to 1$ (plus an exponentially decaying correction), thus yielding $z^* \approx 1+1/\beta \to 1$ which implies $\epsilon_a \to 1$. This latter result is clearly not the correct result for the quenched case as the distribution of the x_i has evolved to permit this maximal energy configuration as explained in the Introduction. Indeed we find from Eq. (28) that $p_a(x) = f_a^2(x) \neq 1$ and becomes peaked at the boundaries.

D. TSP on a ring

When the domain of the one-dimensional TSP is a periodic ring rather than the unit interval with boundaries considered in the last section, the analysis becomes simpler. Moreover, there is an interesting new observable: the winding number. For a ring domain, the shortest path is sometimes the other way round the ring, so the potential is

$$V(x) = \begin{cases} |x|, & \text{for } |x| < \frac{1}{2}, \\ 1-|x|, & \text{for } |x| > \frac{1}{2}. \end{cases} \tag{38}$$

Taking proper account of the contributions from discontinuities in the derivative of this potential, the equivalent formula to Eq. (27) gains a term on the right-hand side:

$$\frac{d^2 f^{(a)}}{dx^2} - \beta^2 f^{(a)}(x) + 2\frac{\beta}{\lambda_a} f^{(a)}(x) = \frac{2\beta e^{-\beta/2}}{\lambda} f^{(a)}(x+1/2), \tag{39}$$

where the eigenfunction is now a periodic function with period 1. In this case, in contrast to the situation with boundaries, the original integral equation (16) admits a constant solution $f_a=1$. For positive β, this must correspond to the largest eigenvalue which is

$$\lambda_a = \frac{2(1-e^{-\beta/2})}{\beta}. \tag{40}$$

The annealed energy per site is then given by

$$\epsilon_a = \frac{1}{\beta} - \frac{1}{2(e^{\beta/2}-1)}. \tag{41}$$

The high-temperature limit of ϵ_a now takes the value $1/4$.

Notice that the constant solution indicates that the annealed density of points is the same as that of the desired quenched distribution, so the annealed approximation is exact in this case. This result follows from the symmetry of the domain and continues to hold for certain other closed domains in higher dimensions. The higher-dimensional cases will be treated in the later section on quenched models.

A new observable, the winding number, arises for this domain. The winding number counts the number of times a particular path goes around the ring and can be written as the sum of contributions from each step between points in the same way as the original Hamiltonian:

$$W(\sigma) = \sum_{i=1}^{N} W(x_{\sigma_i} - x_{\sigma_{i-1}}), \tag{42}$$

where

$$W(x) = \begin{cases} 1+x, & \text{for } x < -\frac{1}{2}, \\ x, & \text{for } |x| < \frac{1}{2}, \\ -1+x, & \text{for } x > \frac{1}{2}. \end{cases} \tag{43}$$

In fact, since the cyclic boundaries lead to $\Sigma(x_{\sigma_i} - x_{\sigma_{i-1}})=0$, the x part of the contributions can be dropped and the winding number may be written:

$$W(\sigma) = \sum_{i=1}^{N} -\theta(x_{\sigma_i} - x_{\sigma_{i-1}} - 1/2) + \theta(-x_{\sigma_i} + x_{\sigma_{i-1}} - 1/2). \tag{44}$$

In this form it shows some similarity with the potential for the descent mode. In particular, the asymmetry will make the right and left eigenfunctions differ.

We compute the expectation values of the winding number by taking the Boltzmann weight of the configuration σ to be

$$\exp[-\beta H(\sigma) - \gamma W(\sigma)]. \tag{45}$$

The analysis developed above holds for this slightly more general case, and we will obtain expectations of the winding number by differentiating the partition function with respect to γ before setting γ to zero.

By considering the equations obtained by differentiating the eigenvalue equation it becomes clear that a solution of the form

$$f_R^a = C \exp(\kappa x) \tag{46}$$

should be sought. Indeed, this form is a solution of the integral equation provided $\kappa = \gamma$. As was the case for the descent model, the left eigenvalue is of the form $f_L^a = C' \exp(-\kappa x)$, so the annealed density becomes constant and this solution is thus also valid for the quenched problem. The corresponding eigenvalue is given by

$$\lambda = \frac{2\beta}{\beta^2 - \gamma^2} - \frac{e^{-\beta/2}}{\beta^2 - \gamma^2}[(\beta + \gamma)e^{\gamma/2} + (\beta - \gamma)e^{-\gamma/2}], \tag{47}$$

which correctly reduces to Eq. (40) when γ is set to zero.

As should be expected, the mean value of the winding number vanishes since there is nothing that prefers winding in one direction over the other. Even in the low-temperature limit, there is no symmetry breaking in this one-dimensional system. On the other hand, the fluctuations provide a nonvanishing observable

$$\langle \overline{W^2} \rangle = \frac{N}{4\beta^2} \frac{8e^{\beta/2} - 8 - 4\beta - \beta^2}{e^{\beta/2} - 1}. \tag{48}$$

In the high-temperature limit the fluctuations per site become $1/12$, and for large negative β the limit is $1/4$.

We have performed Monte Carlo simulations to test this prediction using the quenched model which we have already argued has the same value of observables. These results show good agreement as displayed in Fig. 2.

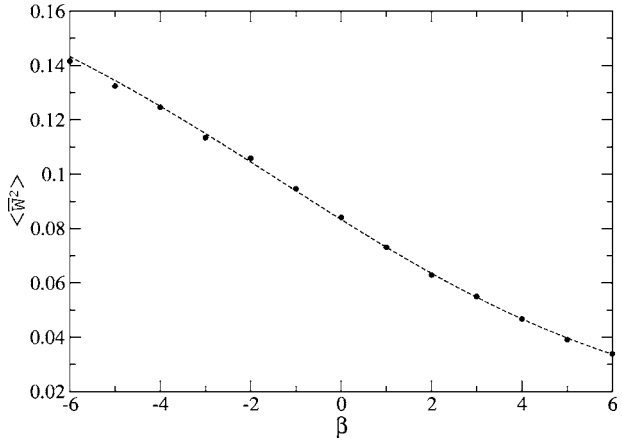

FIG. 2. Expectation value for the fluctuations in winding number per site, $\langle \overline{W^2} \rangle / N$, for the one-dimensional TSP on the ring domain as a function of β (dotted line) compared with the Monte Carlo simulations (crosses). Negative β corresponds to the maximum TSP.

III. QUENCHED CALCULATION

A. General formalism

The order of the points $\mathbf{r}_i$ is unimportant for the statistical mechanics of this problem because the phase space is all their possible orderings. The relevant disorder is thus clearly fully determined by the N position vectors $\mathbf{r}_i$ of the sites. These positions are encoded in the, unaveraged, density of points in space,

$$\rho_q(\mathbf{r}) = \frac{1}{N} \sum_{i=1}^{N} \delta(\mathbf{r} - \mathbf{r}_i^{(q)}), \tag{49}$$

where we have used the superscript q above to emphasize that the points $\mathbf{r}_i^{(q)}$ are quenched. We note that by definition we have $p_q(\mathbf{r}) = \overline{\rho}_q(\mathbf{r})$, and in the limit of large N we expect that

$$\int d^d r\, \rho_q(\mathbf{r}) h(\mathbf{r}) = \int d^d r\, p_q(\mathbf{r}) h(\mathbf{r}) + O(1/\sqrt{N}) \tag{50}$$

for suitably well-behaved functions h. If $\mathbf{r}_i$ is the site visited by the polymer at step i in a system which has $\mathbf{r}_i \in \mathcal{D}$, then the partition function of the permutation problem can be written as

$$Z_N = \frac{1}{N!} \int \prod_{i=1}^{N} d^d r_i \prod_{\mathbf{r}} [N\rho_q(\mathbf{r})]! \prod_{\mathbf{r}} \delta\left(N\rho_q(\mathbf{r}) - \sum_i \delta(\mathbf{r} - \mathbf{r}_i) \right) \times \exp\left(-\beta \sum_i V(\mathbf{r}_{i+1} - \mathbf{r}_i) \right). \tag{51}$$

The above can be derived by considering a discrete version of the problem where one has $n(j)$ sites at the points $\mathbf{r}(j)$. A path is specified by the possible sequences $\mathbf{r}_1, \mathbf{r}_2, \ldots, \mathbf{r}_N$; however, at the visit to the site $\mathbf{r}(j)$ there are $n(j)$ possible points to choose from and thus any path has a degeneracy $\Pi_j n(j)!$ in order to have the same phase space as the permutation problem. In addition each site $\mathbf{r}(j)$ can only be visited $n(j)$ times, explaining the δ-function constraint above. Another way of obtaining the factor in Eq. (51) is to note that $Z_N(\beta) = C_N \Xi_N(\beta)$ where

$$\Xi_N = \int \prod_{i=1}^{N} d^d r_i \prod_{\mathbf{r}} \delta\left(N\rho_q(\mathbf{r}) - \sum_i \delta(\mathbf{r} - \mathbf{r}_i) \right) \times \exp\left(-\beta \sum_i V(\mathbf{r}_{i+1} - \mathbf{r}_i) \right) \tag{52}$$

is the partition function of the system up to a temperature-independent entropy and degeneracy contribution C_N. Clearly, as defined here, $Z(0) = 1$ which implies $Z(\beta) = \Xi(\beta)/\Xi(0)$. We shall see later that, in the limit of large N, we have

$$\Xi_N(0) = \exp\left(- N \int d^d r\, p_q(\mathbf{r}) \{ \ln[p_q(\mathbf{r})] - 1 \} \right), \quad (53)$$

which in the large N limit, via Stirling's formula, recovers Eq. (51).

The partition function Ξ_N may be written using a Fourier representation of the functional constraint:

$$\Xi_N = \int d[\mu] \exp\left(N \int d^d r\, \mu(\mathbf{r}) \rho_q(\mathbf{r}) \right) \mathcal{Z}_N, \quad (54)$$

where each integration over $\mu(x)$ is up the imaginary axis. The object $\mathcal{Z}_N$ is similar to the annealed partition function considered in the previous section, but with an $\mathbf{r}$-dependent chemical potential. It is defined as

$$\mathcal{Z}_N = \int \prod_{i=1}^{N} d^d r_i \exp\left(- \beta \sum_{i=1}^{N} V(\mathbf{r}_i - \mathbf{r}_{i-1}) - \sum_{i=0}^{N} \mu(\mathbf{r}_i) \right). \quad (55)$$

For large N we may use relation (50), neglect the terms $O(\sqrt{N})$, and then the partition function in Eq. (54) can be evaluated by the saddle point method in the limit where $N \to \infty$ keeping $\mathcal{D}$ fixed. The saddle point equation is

$$\begin{aligned} p_q(\mathbf{r}) &= - \frac{1}{N} \frac{\delta \ln \mathcal{Z}_N}{\delta \mu(\mathbf{r})} \\ &= \frac{1}{N} \left\langle \sum_{i=1}^{N} \delta(\mathbf{r} - \mathbf{r}_i) \right\rangle \\ &= p_a(\mathbf{r}) = - \frac{\delta \ln(\lambda_q)}{\delta \mu(\mathbf{r})}, \end{aligned} \quad (56)$$

where the above expectation is in the system with partition function $\mathcal{Z}_N$ defined in Eq. (55).

Physically this approach can be thought of as choosing a site-dependent chemical potential μ which fixes the density of the annealed calculation to be the same as that of the quenched one, $p_q(\mathbf{r}) = p_a(\mathbf{r})$. This idea was used sometime ago in an approximative sense where low-order moments, not the whole distribution, were fixed in this way [18,19].

To proceed, we find an expression for $p_a(\mathbf{r})$ using similar techniques to those employed in the last section. We find

$$\mathcal{Z}_N = \mathrm{Tr}\, \mathcal{T}^N, \quad (57)$$

where

$$\mathcal{T}(\mathbf{r}, \mathbf{r}') = \exp[-\mu(\mathbf{r})/2] \exp[-\beta V(\mathbf{r} - \mathbf{r}')] \exp[-\mu(\mathbf{r}')/2]. \quad (58)$$

The right and left ground-state eigenfunctions, corresponding to the maximal eigenvalue λ_q, obey

$$f_R^{(q)}(\mathbf{r}) = \lambda_q^{-1} \exp[-\mu(\mathbf{r})/2] \int d^d r' \exp[-\beta V(\mathbf{r} - \mathbf{r}')] \times \exp[-\mu(\mathbf{r}')/2] f_R^{(q)}(\mathbf{r}'), \quad (59)$$

$$f_L^{(q)}(\mathbf{r}) = \lambda_q^{-1} \exp[-\mu(\mathbf{r})/2] \int d^d r' \exp[-\beta V(\mathbf{r}' - \mathbf{r})] \times \exp[-\mu(\mathbf{r}')/2] f_L^{(q)}(\mathbf{r}'), \quad (60)$$

and by a similar calculation to that of the annealed case we have

$$p_q(\mathbf{r}) = p_a(\mathbf{r}) = - \frac{\delta \ln(\lambda_q)}{\delta \mu(\mathbf{r})} = f_R^{(q)}(\mathbf{r}) f_L^{(q)}(\mathbf{r}). \quad (61)$$

In the case of a symmetric potential where $V(\mathbf{r}) = V(-\mathbf{r})$, we have that $f_R^{(q)} = f_L^{(q)} = f^{(q)}$ and thus $f^{(q)} = \sqrt{p_q}$. Note that this ensures that $f^{(q)}$ is the eigenfunction corresponding to the maximal eigenvalue as we note that it is positive and then appeal to the Perron-Frobenius theorem. Substituting the above into the saddle point equation gives

$$\sqrt{p_q(\mathbf{r})} = \lambda_q^{-1} \exp\left(- \frac{\mu(\mathbf{r})}{2} \right) \int d^d r' \exp[-\beta V(\mathbf{r} - \mathbf{r}')] \times \exp\left(- \frac{\mu(\mathbf{r}')}{2} \right) \sqrt{p_q(\mathbf{r}')}. \quad (62)$$

We can thus write $\exp[-\mu(\mathbf{r})/2] = \sqrt{p_q(\mathbf{r})}/s_{\lambda_q}(\mathbf{r})$ where $s_{\lambda_q}(\mathbf{r})$ obeys

$$s_{\lambda_q}(\mathbf{r}) = \lambda_q^{-1} \int d^d r' \exp[-\beta V(\mathbf{r} - \mathbf{r}')] \frac{p q(\mathbf{r}')}{s_{\lambda_q}(\mathbf{r}')}. \quad (63)$$

Substituting this back into the action we obtain

$$\frac{\ln(Z_N)}{N} = 2 \int d^d r\, p_q(\mathbf{r}) \ln[s_{\lambda_q}(\mathbf{r})] + \ln(\lambda_q) - \int d^d r\, p_q(\mathbf{r}) \ln[p_q(\mathbf{r})]. \quad (64)$$

The last term which is independent of β explains the presence of the combinatorial term in Eq. (51). However, from Eq. (63) we see that there is a whole family of solutions $\{s_{\lambda_q}(\mathbf{r}), \lambda_q\}$ which are related by $s_{\lambda_q} = a^{1/2} s_{a\lambda_q}$ for $a > 0$, and in addition these solutions all have the same action. This apparent zero mode is an artifact introduced by the fact that the constraint $N \int d^d r\, \rho_q = \int d^d r \sum_i \delta(\mathbf{r} - \mathbf{r}_i)$ is automatically satisfied. Thus we may choose $\lambda_q = 1$. In the case of a uniform distribution on a domain of unit volume this leads to our final result

$$\begin{aligned} \epsilon &= - 2 \frac{\partial}{\partial \beta} \left[\int d^d r \ln[s(\mathbf{r})] \right] \\ &= \int d^d r\, d^d r' \frac{V(\mathbf{r} - \mathbf{r}') \exp[-\beta V(\mathbf{r} - \mathbf{r}')]}{s(\mathbf{r}) s(\mathbf{r}')}, \end{aligned} \quad (65)$$

where s obeys

$$s(\mathbf{r}) = \int d^d r' \frac{\exp[-\beta V(\mathbf{r} - \mathbf{r}')]}{s(\mathbf{r}')} \quad (66)$$

and we have specialized to the usual case when the distribution of quenched points is uniform. Recall that we have set

the size of the domain to 1, and some scaling is needed when this is not the case.

It is possible to check our result via direct comparison with the high-temperature expansion, Eq. (22), given at the end of Sec. II. Equation (66) can be solved perturbatively as a power series in β by writing

$$s(\mathbf{r}) = 1 + \beta s_1(\mathbf{r}) + \beta^2 s_2(\mathbf{r}) + \cdots . \tag{67}$$

Substituting this expansion into Eq. (66) yields

$$s_1(\mathbf{r}) = -\int d^d r'\ V(\mathbf{r}-\mathbf{r}') + \frac{1}{2}\int d^d r'\ d^d r''\ V(\mathbf{r}''-\mathbf{r}'), \tag{68}$$

$$\begin{aligned} s_2(\mathbf{r}) = {} & \frac{1}{2}\int d^d r'\ V^2(\mathbf{r}-\mathbf{r}') + \int d^d r'\ s_1(\mathbf{r}')V(\mathbf{r}-\mathbf{r}') \\ & - \frac{1}{4}\int d^d r'\ dz\ V^2(\mathbf{r}'-z) \\ & - \frac{1}{2}\int d^d r'\ d^d r''\ s_1(\mathbf{r}')V(\mathbf{r}'-\mathbf{r}'') + \frac{1}{2}\int d^d r'\ s_1(\mathbf{r}'). \end{aligned} \tag{69}$$

To order β, Eq. (65) then yields

$$\epsilon = -2\int d^d r\left[s_1(\mathbf{r}) + 2\beta\left(s_2(\mathbf{r}) - \frac{s_1^2(\mathbf{r})}{2}\right)\right] + O(\beta^2), \tag{70}$$

and substituting Eqs. (69) and (69) in the above we recover the result, Eq. (22).

B. Quenched Rouse polymer

Before moving on to consider the TSP, we first analyze a model with a harmonic potential to demonstrate an analytic solution of the quenched equations. This system, in the annealed case, is used to model a polymer [13]. To avoid boundaries, which prevent an analytic solution, we treat the case where the quenched distribution of points is Gaussian, $p_q(r) = e^{-r^2/2}/(2\pi)^{d/2}$, and we work in arbitrary dimension d. The quenched equation for $s(\mathbf{r})$ becomes

$$s(\mathbf{r}) = \int \frac{d^d r'}{(2\pi)^{d/2}} \frac{e^{-r'^2/2}\exp(-\beta|\mathbf{r}-\mathbf{r}'|^2)}{s(\mathbf{r}')}. \tag{71}$$

So we search for a Gaussian solution

$$s(\mathbf{r}) = s e^{-\gamma r^2/2}. \tag{72}$$

This is satisfied provided

$$\gamma = \frac{1}{2}(1 + 2\beta - \sqrt{1+4\beta^2}), \tag{73}$$

$$s = 2^{d/4}(1+\sqrt{1+4\beta^2})^{-d/4}. \tag{74}$$

Inserting these into the saddle point action we obtain the average energy per site as

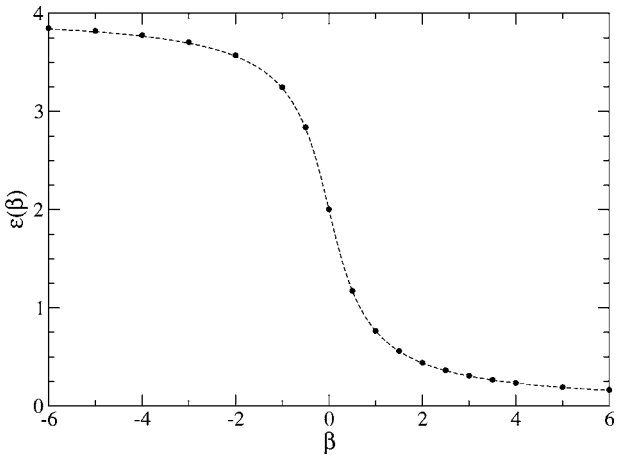

FIG. 3. Theoretical prediction for the average energy ϵ for the two-dimensional quenched polymer model as a function of β (solid line) compared with the Monte Carlo simulations (solid circles). Negative β corresponds to the maximal problem. Error bars based on 20 realizations of the quenched points are smaller than the symbol sizes. Here the domain $\mathcal{D}$ is unbounded but p_q is Gaussian and centered at the origin.

$$\epsilon = d\left(1 - \frac{2\beta}{\sqrt{1+4\beta^2}} + \frac{2\beta}{\sqrt{1+4\beta^2}(1+\sqrt{1+4\beta^2})}\right). \tag{75}$$

This has the correct $d/2\beta$ behavior at large β and the value $\epsilon = d$ at infinite temperature, as can be checked directly by a Gaussian average. In contrast to the situation for directed polymers, there is no evidence for a phase transition in this quenched case.

In Fig. 3 we show the average energy in the two-dimensional case and compare it with Monte Carlo simulations. The agreement is good, although it should be noted that at the edges of the plot, for large $|\beta|$, long runs (tens of millions of steps) with large N are required to see accurate agreement.

C. TSP in one and two dimensions

In this section we consider predictions for the TSP in both one and two dimensions. In view of the nonlinear nature of Eqs. (65) and (66) we have not found any nontrivial analytic solutions for the TSP potential. Our primary tool is the iterative numerical solution of Eq. (66) which is stable and can be solved to any required accuracy. However, for closed symmetric domains (we shall consider a one-dimensional ring and a disk and torus in two dimensions), a constant solution exists and some analytic progress is possible. To see this, we simply require a domain such that that the origin of the integration in Eq. (66) can be shifted to yield

$$s^2 = \int d^d r \exp[-\beta V(\mathbf{r})]. \tag{76}$$

The significance of this observation is that the annealed approximation is exact for these domains. Indeed this equation is exactly the annealed eigenvalue equation for a constant eigenfunction and the relationship between the value of the

constant s and the eigenvalue λ of the annealed approximation is simply $\lambda=s^2$. In all cases the normalization is $\lambda(\beta=0)=1$. This conclusion is consistent with what is known from analysis of the independent link version of the TSP. Evidently, the geometry of independent links has no boundaries and the analysis of this problem in the same scaling limit we consider here also shows that that the annealed approximation is exact [7].

Expression (76) allows a general large-β expansion for these closed domains. Provided the potential is convex, then in this limit it is apparent that the only contribution to the integral is from nearby points. When the potential is smooth we can expand to find $\lambda \sim e^{-\beta V(0)}(\beta V'')^{-d/2}$, so the energy is $\epsilon \sim V(0)+d/2\beta$. This expansion is invalid for the TSP (and descent model) since the potential is not smooth and the correct energy is $\epsilon \sim d/\beta$. These results indicate that in this limit the topology of the domain becomes unimportant and only the dimension is relevant as is indeed observed in all the examples below. A similar limit for the maximal problem is dominated by a term corresponding to the largest distance two points can be apart from each other, which is sensitively dependent on the topology of the domain.

1. One dimension

For the case of the ring domain, constant s is a solution and as expected this reproduces the energy obtained via the annealed calculation (41).

For the unit interval, we use Eq. (65) to predict the energy by iteratively solving Eq. (66).

To test these predictions we have carried out Monte Carlo simulations of the TSP for system sizes of $N=5000$ and compared the average energy measured after equilibrating the system over 500 Monte Carlo sweeps and measuring the average energy over a subsequent 500 Monte Carlo sweeps. The disorder average was carried out by averaging the results over 20 independent realizations of the disorder. The standard move was taken to be a random transposition of a pair of points in the permutation, and the acceptance of the move was chosen with the Metropolis rule. The results for both the ring and line domains are shown in Fig. 4 compared with the predictions. We see that for all temperatures the agreement is excellent.

In the same figure we also show the result for the annealed approximation for the line domain based on Eqs. (33)–(36). We see that this provides a lower energy than the quenched result for positive β and higher for negative β.

The fluctuation in the energy $\langle(\epsilon-\langle\epsilon\rangle)^2\rangle$ at high temperature can be computed using the order-β term in Eq. (22). This takes different values for annealed and quenched cases, but agrees in each case with the respective values computed using the combinatorial approach of Ref. [16].

2. Two dimensions

In two dimensions the domains we consider are the sphere, torus, and unit square or box.

It is convenient to treat a sphere of unit radius, so the basic equations need a little modification to deal with a domain $\mathcal{D}$ whose size is not one but $\mathcal{V}$. In effect, all integrals

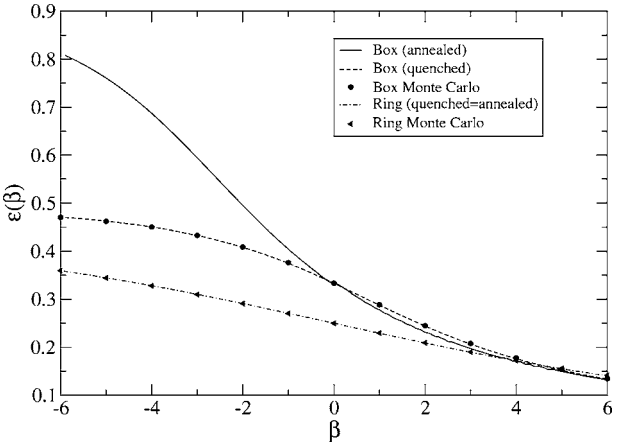

FIG. 4. Theoretical prediction for the average energy ϵ for one-dimensional TSP on ring and line domains as a function of β (solid line) compared with the Monte Carlo simulations (solid circles). The results of the annealed approximation for the line domain is also shown. Negative β corresponds to the maximum TSP. Error bars based on 20 realizations of the quenched points are smaller than the symbol sizes.

appearing in the formalism are normalized by the volume and the final expression for the energy $E(\beta,\mathcal{V})$ scales as

$$E(\beta,1)=\frac{1}{\mathcal{V}^{1/d}}E(\beta/\mathcal{V}^{1/d},\mathcal{V}). \tag{77}$$

The annealed and quenched equations have a constant solution with

$$\lambda=s^2=\frac{1}{4\pi}\int_{S_2} d^2\, r\, e^{-\beta\theta}=\frac{1}{2(\beta^2+1)}(1+e^{-\pi\beta}), \tag{78}$$

leading to energy (normalized for a unit size domain)

$$\epsilon_a=\frac{2\beta}{\beta^2+4\pi}+\frac{\sqrt{\pi}}{2(e^{\sqrt{\pi}\beta/2}+1)}. \tag{79}$$

Note that in the limit $\beta\to-\infty$, the energy becomes the half circumference, corresponding, as is the case for all the closed domains, to the maximum distance two points can be apart.

For a torus we return to unit-size domain normalization and find that the annealed and quenched equations yield

$$\lambda=s^2=\frac{8}{\beta^2}\int_0^{\pi/4}\left(1-e^{(-\beta/2\cos(\theta))}-\frac{\beta e^{(-\beta/2\cos(\theta))}}{2\cos\theta}\right)d\theta$$
$$=\frac{2\pi}{\beta^2}-\frac{8}{\beta^2}\int_0^{\ln(1+\sqrt{2})}\left(\frac{1+(\beta/2)\cosh v}{\cosh v}e^{(-\beta/2)\cosh v}\right)dv. \tag{80}$$

In the high-temperature limit the integral can be evaluated analytically, leading to

$$\epsilon_a(\beta=0)=\frac{1}{6}[\sqrt{2}+\ln(1+\sqrt{2})]=0.382597858. \tag{81}$$

At very low temperature we can do a saddle point near $v=0$ in the second version of the integral. This gives λ

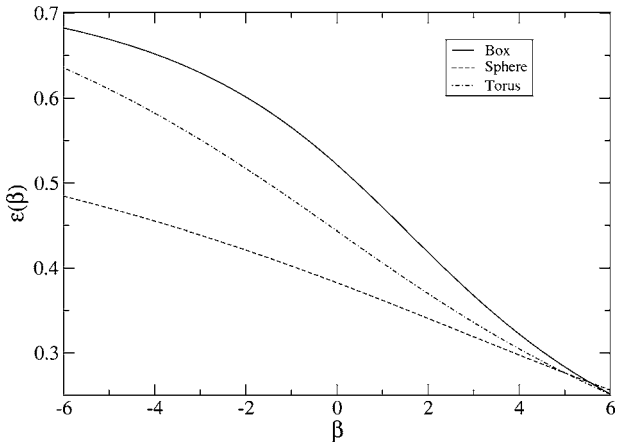

FIG. 5. Theoretical prediction for the average energy ϵ for the two-dimensional TSP on a sphere, box, and torus as a function of β. Negative β corresponds to the maximum TSP.

$\rightarrow 2\pi/\beta^2$ and $\epsilon \rightarrow 2/\beta$. The same result comes more simply from realizing that only short distances contribute in the original two-dimensional integral. A similar argument can be used for large negative β to give $\lambda \rightarrow 8e^{\beta/\sqrt{2}}/\beta^2$ and $\epsilon \rightarrow 1/\sqrt{2} - 2/|\beta|$.

For the traditional TSP on a unit-square domain, the quenched result is different from the annealed approximation and there is little hope of a general analytic solution. Particular values, such as the high-temperature $\beta=0$ value, may be evaluated (given patience with a 4D integral). In a later section we derive expansions for large $|\beta|$.

Figure 5 shows the average energy for each of the three domains. For the sphere this is given by Eq. (79), for the torus it is based on numerical integration of Eq. (80), and for the box we resort to an iterative solution of the original quenched equations. The accuracy of this iterative technique is confirmed by reproducing the results for the other domains. In all these cases we have also performed Monte Carlo simulations and obtain excellent agreement with the theory. At large positive β the topology starts to become unimportant and each domain has energy $\sim 2/\beta$ as expected for a two-dimensional TSP.

D. Descent model

In the case of the descent model, $V(x)$ is clearly not an even function of x, and the general approach presented above does not apply; however, the value of λ_q as a functional of μ can be explicitly computed. Despite the fact that we know the annealed approximation produces the correct result we shall pursue our method in this case as it is rather instructive to do so.

Defining $R(x) = \int_0^x \exp[-\mu(y)/2] f_R^{(q)}(y) dy$ in Eq. (60) we find

$$\exp(-\mu)\frac{dR}{dx} = \lambda_q^{-1}\{[1-\exp(-\beta)]R(x) + \exp(-\beta)R(1)\}. \tag{82}$$

Now we define $y(x) = \int_0^x dy \exp[-\mu(y)]$ to obtain

$$\frac{dR}{dy} = \lambda_q^{-1}\{[1-\exp(-\beta)]R(y) + \exp(-\beta)R(y(1))\}. \tag{83}$$

This can be solved giving

$$[\exp(\beta)-1]\frac{R(y(x))}{R(y(1))} + 1 = \exp\{\lambda_q^{-1} y(x)[1-\exp(-\beta)]\}. \tag{84}$$

Now setting $x=1$ in the above gives

$$\exp(\beta) = \exp\{\lambda_q^{-1} y(1)[1-\exp(-\beta)]\}, \tag{85}$$

which yields

$$\lambda_q = \frac{1-\exp(-\beta)}{\beta}\int_0^1 dy \exp[-\mu(y)]. \tag{86}$$

We thus find that

$$-\frac{\delta \ln(\lambda_q)}{\delta \mu(x)} = \frac{\exp[-\mu(x)]}{\int_0^1 dy \exp[-\mu(y)]}. \tag{87}$$

A solution (there is again a family related by a constant factor giving the same action) to the saddle point equation is

$$\exp[-\mu(x)/2] = \sqrt{p_q(x)}. \tag{88}$$

This now yields

$$\frac{\beta F_N}{N} = -\ln[1-\exp(-\beta)] + \ln(\beta) + \text{terms independent of } \beta. \tag{89}$$

This is the same result as the annealed calculation of the precedent section as expected.

E. Other one-dimensional potentials

As an additional numerical verification of our method we have considered the potentials $V(x)=x^2$ and also $V(x)=-\ln(|x|)$ on the line domain $\mathcal{D}=[0,1]$. The latter potential was only considered at positive temperature as it is ill defined at negative temperature. The comparison of the predictions of our method against results obtained from Monte Carlo simulations (carried out with the same protocols as for the TSP case) are shown in Figs. 6 and 7. The agreement is again excellent.

IV. GENERAL ZERO-TEMPERATURE BEHAVIOR IN ONE DIMENSION

In some one-dimensional cases we may analyze the low-temperature behavior of Eq. (66) and extract the low-temperature energy of the system analytically. We write $s(x) = \exp[-\beta w(x)] t(x)$, and thus Eq. (66) becomes

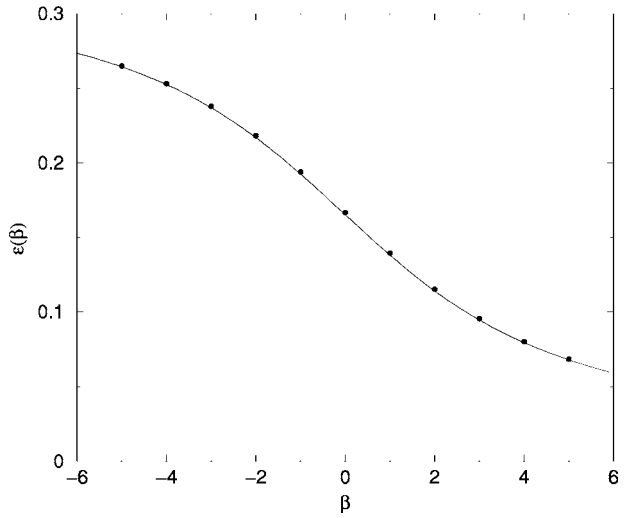

FIG. 6. Predicted average energy for potential $V(x)=x^2$ as a function of β (solid line) against values measured from Monte Carlo simulations (solid circles).

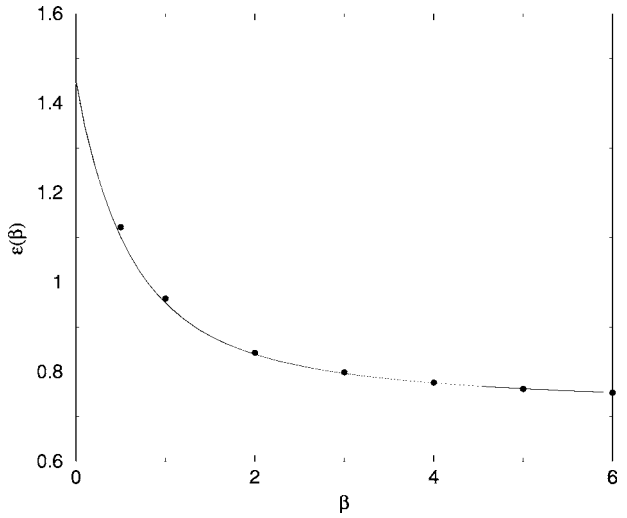

FIG. 7. Predicted average energy for potential $V(x)=-\ln(|x|)$ as a function of β (solid line) against values measured from Monte Carlo simulations (solid circles).

$$\exp[-\beta w(x)]t(x) = \int dy \frac{\exp[-\beta V(x-y)+\beta w(y)]}{t(y)}. \tag{90}$$

We now assume that $\ln[t(x)]/\beta \to 0$ as $\beta \to \infty$ which permits us to evaluate the integral on the right-hand side of Eq. (90) via the saddle point method:

$$\exp[-\beta w(x)]t(x) \approx \exp[-\beta r(x)] \int_{-\infty}^{\infty} d\zeta \times \exp\left[-\frac{\beta\zeta^2}{2}[V''(x-x^*(x)) - w''(x^*(x))]\right], \tag{91}$$

where

$$r(x) = V(x-x^*(x)) - w(x^*(x)) = \min_{y\in(0,1)} \{V(x-y) - w(y)\}, \tag{92}$$

and the point $x^*(x)$ is simply the point about which the action in the saddle point is minimal, the fluctuations being integrated about this point. It is at this point tempting to suggest a tentative physical interpretation of $x^*(x)$ as the optimal point that the polymer jumps to if its current position is x; that is to say, if the monomer i is at x, then the optimal position for monomer $i+1$ is at $x^*(x)$.

The function $w(x)$ is thus determined by $r(x)=w(x)$—i.e.,

$$w(x) = \min_{y\in(0,1)} \{V(x-y) - w(y)\}. \tag{93}$$

Intriguing we will see that by effectively guessing some (local) heuristics for $x^*(x)$ we will be able to obtain some solutions to Eq. (93). Putting all this together we obtain the equation for t:

$$t(x)t(x^*(x)) = \left(\frac{2\pi}{\beta[V''(x-x^*(x)) - w''(x^*(x))]}\right)^{1/2}, \tag{94}$$

this only being valid if $V''(x-x^*(x)) - w''(x^*(x)) > 0$ on all but a set of measure zero and when, again on all but a set of measure zero, the minimizing point occurs within the domain [0,1]. To simplify our analysis we shift the domain [0,1] to the domain $[-\frac{1}{2},-\frac{1}{2}]$; by symmetry, we now expect that $w(x)=w(-x)$ and $t(x)=t(-x)$. The shifted equation for w is simply

$$w(x) = \min_{y\in(-1/2,1/2)} \{V(x-y) - w(y)\}. \tag{95}$$

The energy is now given by

$$\epsilon \approx 2\int_{-1/2}^{1/2} dx w(x) - 2\frac{\partial}{\partial\beta}\int_{-1/2}^{1/2} dx \ln[t(x)]. \tag{96}$$

If indeed $x^*(x)$ is the point which is the optimal to jump to from x, we expect a one-to-one correspondence between x and $x^*(x)$ in order to generate a uniform annealed distribution. If this is indeed the case, then for any function F on [0,1] we will have

$$\int dx\, F(x) = \int dx\, F(x^*(x)). \tag{97}$$

Using Eq. (97) and Eqs. (96) and (94) we find

$$\epsilon \approx 2\int_{-1/2}^{1/2} dx\, w(x) - \frac{\partial}{\partial\beta}\int_{-1/2}^{1/2} dx \ln[t(x)t(x^*(x))] = 2\int_{-1/2}^{1/2} dx\, w(x) + \frac{1}{2\beta}. \tag{98}$$

Thus, given that the conditions stated above all hold, the correction to the zero-temperature energy at low temperatures takes a remarkably universal form.

We first consider the case where V is a purely attractive potential with a minimum at $x=0$. Taking the idea that $x^*(x)$ is the optimal jump from the point x we expect $x^*(x)=x$. This will imply from Eq. (93) that $w(x)=V(0)/2$. This solution can be seen to work when plugged back into Eq. (93) when $V'(0)=0$ and $V''(0)>0$. We thus find from Eq. (98) that

$$\epsilon \approx V(0) + \frac{1}{2\beta}. \tag{99}$$

We now consider the case where the potential is everywhere repulsive. On the interval $[-\frac{1}{2},\frac{1}{2}]$ the greedy algorithm described earlier amounts to making the choice $x^*(x)=-x$. This choice implies that

$$w(x) = V(2x) - w(x), \tag{100}$$

and for the solution to be valid we must have that

$$-V'(2x) - w'(-x) = 0. \tag{101}$$

If $w(x)=w(-x)$, then we have $w'(x)=-w'(-x)$ and so the above implies that $w(x)=V(2x)/2$. For this solution to be valid we must have that $V''(2x)<0$ and thus it only holds for concave potentials.

The low-temperature energy is thus given by

$$\epsilon = \int dx\, V(x) + \frac{1}{2\beta}. \tag{102}$$

The ground-state energy is clearly that given by the greedy algorithm

$$\epsilon_{GA} = \int dx\, V(x). \tag{103}$$

Another heuristic for finding the maximal path in the case of repulsive potentials is to take a jump size of constant size Δ. When there are no minima the best value for Δ is $1/2$; this strategy clearly minimizes the energy at each jump subject to the constraint that it must be possible from any position x. One simply adds a very small noise η to each jump of $1/2$ to generate the required uniform distribution of monomers on $[0,1]$. We call this the half-jump algorithm, and it is clearly not at all greedy. We thus take $x^*(x)$ so that $|x-x^*(x)|=1/2$. When $x>0$ this implies $x^*(x)=x-1/2$ and hence

$$w(x) = V\left(\frac{1}{2}\right) - w\left(x-\frac{1}{2}\right). \tag{104}$$

The explicit solution to this equation is $w(x)=a|x|+b$, where

$$b = V\left(\frac{1}{2}\right) - \frac{a}{2} - b, \tag{105}$$

and the condition to have a minimum implies that

$$V'\left(\frac{1}{2}\right) - a = 0 \tag{106}$$

and $V''(1/2)>0$. Thus the function V cannot be concave near $x=1/2$ and

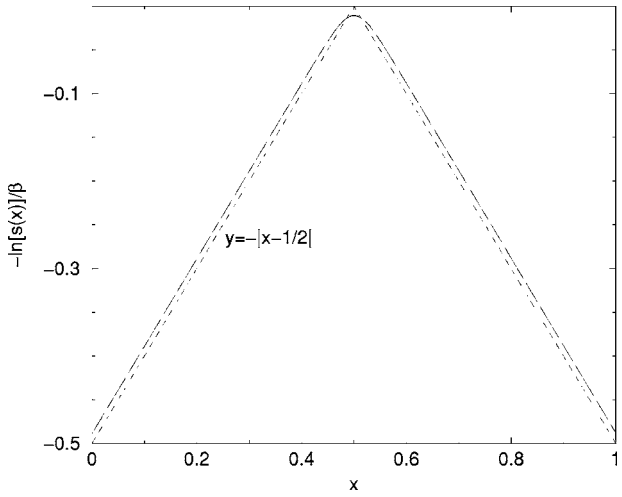

FIG. 8. Value of $-\ln[s(x)]/\beta$ obtained by numerically solving Eq. (66) at $\beta=30$ (solid line) for the potential $V(x)=-|x|$. Also is shown the zero-temperature prediction for this function (dashed line).

$$b = \frac{1}{2}\left[V\left(\frac{1}{2}\right) - \frac{1}{2}V'\left(\frac{1}{2}\right)\right]. \tag{107}$$

As expected this solution gives

$$\epsilon = V\left(\frac{1}{2}\right) + \frac{1}{2\beta}, \tag{108}$$

which is obviously the ground-state energy given by the half-jump algorithm energy.

A potential where the above solution is possible is $V(x)=-\ln(|x|)$. Numerical solution of Eq. (66) at low temperatures converges to the solution found above. The predicted value of the ground-state energy is $\epsilon_{GS}=\ln(2)$; this value is compatible with the Monte Carlo simulations for this potential shown in Fig. 7. Clearly the greedy algorithm is a bad strategy for the potential $V(x)=-\ln(|x|)$; this is because at the end it must link points very close to each other situated near $x=1/2$, thus giving a very large contribution to the energy at the end of the algorithm. The greedy algorithm gives an energy $\epsilon=-\int dx \ln(x)=1$, which is indeed higher than the ground state we predict analytically and not compatible with our Monte Carlo simulations. When $V''(|x|)>0$ everywhere in $[0,1]$, Jensen's inequality tells us that $\langle V(X)\rangle \geqslant V\langle X\rangle$ for X distributed on $[0,1]$; when this distribution is uniform this implies that $\epsilon_{GA}>\epsilon_{HA}$ and hence the half-jump algorithm is the most efficient. In the case where the potential is concave the greedy algorithm is the most efficient.

We note that the case of the maximum TSP is an intermediate case where $V''(x)=0$, and in this case $\epsilon_{GA}=\epsilon_{HA}$ and the forms of $u(x)$ in these two cases coincide. As a check of this asymptotic analysis we have numerically solved Eq. (66) for the potential $V(x)=-|x|$ at $\beta=30$. Shown in Fig. 8 is $w^*(x)=-\ln[s(x)]/\beta$ where $s(x)$ is the numerical solution of Eq. (66) at $\beta=30$. Also shown is the predicted zero-temperature limit of w^*. The agreement improves on increasing β but

limitations of numerical accuracy are attained if β is taken to be too large.

The finite-temperature corrections for both the TSP and maximum TSP are different from those of the cases considered thus far as $V''(x)=0$ for $x\neq 0$. At positive temperature it is clear that $w(x)=0$, as the saddle point is at $x^*(x)=x$. Here, because $V''(x)=0$, we do not expand the terms in the exponential of the integral about $y=0$ but we do carry out the expansion of the term $1/t(y)$; we thus write

$$t^2(x) \approx \int_{-1/2}^{1/2} dx \exp(-\beta|x-y|) = \frac{1}{\beta}\left[2-\exp\left(-\frac{\beta}{2}-\beta x\right)-\exp\left(-\frac{\beta}{2}+\beta x\right)\right]. \tag{109}$$

As $\beta\to\infty$ we have

$$\int dx \ln[s(x)] \approx \int_0^{1/2} dx \ln\left(1-\frac{1}{2}\exp(-\beta x)\right)+\frac{1}{2}\ln\left(\frac{2}{\beta}\right) \approx \frac{1}{2\beta}\left[-\frac{\pi^2}{6}+\ln^2(2)\right]+\frac{1}{2}\ln\left(\frac{2}{\beta}\right). \tag{110}$$

This yields

$$\epsilon \approx \frac{1}{\beta}-\frac{1}{\beta^2}\left(\frac{\pi^2}{6}-\ln^2(2)\right) \tag{111}$$

for the TSP as $\beta\to\infty$. We have checked that this result agrees with the asymptotics of our numerical solutions.

The analysis for the maximum TSP is more involved. Differentiating Eq. (65) twice we see that the function $s(x)$ obeys

$$s''(x)=\beta^2 s(x)+\frac{2\beta}{s(x)}. \tag{112}$$

We now make the substitution $s(x)=\exp(\beta|x|)t(x)$ to find

$$t''(x)+2\beta\,\mathrm{sgn}(x)t'(x)=-2\beta\delta(x)t(0)+\frac{2\beta\exp(-2\beta|x|)}{t(x)}. \tag{113}$$

Now in the limit $\beta\to\infty$ we have $2\beta\exp(-2\beta|x|)\approx\delta(x)$. For large β we thus have

$$t''(x)+2\beta\,\mathrm{sgn}(x)t'(x)=\delta(x)\left(-2\beta t(0)+\frac{1}{t(0)}\right). \tag{114}$$

The above has solution $t(x)=A+B\exp(-2\beta|x|)$, and the jump conditions at the origin yield the relation

$$A^2-B^2=\frac{1}{2\beta}. \tag{115}$$

An extra relation between A and B is found from examining the integral equation for t at $x=0$, which in this limit gives

$$A+B=\frac{1}{A}, \tag{116}$$

and in the limit of large β we find $A\approx B\approx 1/\sqrt{2}$ and we find that the large-β behavior of the energy is

$$\epsilon \approx -\frac{1}{2}+\frac{\pi^2}{6\beta^2}. \tag{117}$$

To end our analysis of the low-temperature limit we will consider the maximum TSP in higher (d) dimensions, specifically on the hypercube $[0,1]^d$. Consider the generalization of the greedy heuristic. Here we start on the outermost layer of points in the hypercube and we join points on this surface to those that are diametrically opposed. The procedure is then repeated eroding the hypercube until we arrive at the center. Shifting the domain to $\left[-\frac{1}{2},\frac{1}{2}\right]^d$ as before, this entails matching the point x with $-x$. This generalized heuristic was shown to give the optimal path length for $d=2$ [20]. The ground-state energy generated by this generalized greedy heuristic is clearly

$$\epsilon_{GA}=2^d\int_{[0,1/2]^d} dx\, V(2x)=-2^{d+1}\int_{[0,1/2]^d} dx\,|x|. \tag{118}$$

This general formula gives $\epsilon_{GA}=-0.5$, $-0.765\,196$, and $-0.960\,592$ in one, two, and three dimensions, respectively. The solution $w(x)=-x$ is in fact a solution to Eq. (93) and thus gives these ground-state energies. This can be easily verified as we note that the function

$$h(x)=|y|-|x-y| \tag{119}$$

is bounded as

$$h(x)\geqslant -|x| \tag{120}$$

by the triangle inequality. The bound is achieved at $y=-x$, confirming that $w(x)=-x$ is indeed a solution. We note that this solution exists in any domain $\mathcal{D}$ (centered at the origin) satisfying the property that if $x\in\mathcal{D}$, then $-x\in\mathcal{D}$.

V. CONCLUSIONS

We have discussed the statistical mechanics of models whose phase space is the set of permutations of N objects characterized by quenched positions $\mathbf{r}_i$. The Hamiltonians are functions of the neighboring elements in the sequence, and thus a given sequence can be interpreted as the energy of a polymer ring or closed random walk which visits all points in the quenched distribution once. We analyzed the cases corresponding to several well-studied problems including the traveling salesman problem, the descent problem, and the quenched Rouse model.

The annealed approximation was first considered and illustrated for some one-dimensional cases. For the TSP on a ring and the descent problem this annealed approximation gives the correct quenched result. For the descent model, this is because the effective potential between neighboring monomers, when the system is viewed as a polymer with interac-

tions between consecutive monomers, is scale free and independent of the quenched distribution of the random points. For the TSP on a ring, the reason is less clear, but agrees with expectations from replica studies of the independent-link approximation and continues to hold for symmetric closed domains in higher dimensions. However, in general, we expect the annealed approximation to fail at all but infinite temperature. This is because the points $\mathbf{r}_i$ are allowed to evolve dynamically to lower the free energy of the system and the resulting thermodynamic distribution will not be the same as their original quenched distribution.

We then showed how the quenched calculation could be carried out and confirmed its predictions for both one- and two-dimensional TSP examples with Monte Carlo simulations. Physically the method we introduced corresponds to imposing a fictitious site-dependent chemical potential on the distribution of a set of dynamical variables $\mathbf{r}_i$ in the presence of the original interaction Hamiltonian. This chemical potential is then chosen to ensure that the annealed distribution of the positions of these dynamical $\mathbf{r}_i$, denoted in this paper by $p_a(\mathbf{r})$, is the same as the quenched distribution of the quenched random variables $\mathbf{r}_i^{(q)}$ denoted by $p_q(\mathbf{r})$. The method is exact in the thermodynamic limit (corresponding to high density where the length of the interval is held constant) for any quenched distribution $p_q(\mathbf{r})$ and interaction potential $V(\mathbf{r})$. One of the most intriguing observations made here is that in the annealed approximation we are led to consider a linear eigenvalue problem to solve the thermodynamics as we use a transfer matrix approach; however, in the quenched calculation we are led to consider a nonlinear integral equation. Although we managed to avoid the sometimes rather opaque replica method in our treatment, it would be interesting to see if the appearance of the nonlinear eigenvalue equation could be interpreted or rederived within the replica formalism. The results of our calculations were then confirmed by comparing them with Monte Carlo simulations in a variety of models. In the cases we have considered so far we have seen no evidence for any phase transition on lowering the system's temperature. It is possible, however, that in higher dimensions and with certain interaction potentials V a phase transition does occur. We recall that a directed polymer in dimensions greater than 2 exhibits a finite-temperature phase transition [21].

Particular attention was paid to the zero-temperature limit where Eq. (93) needs to be solved. A number of solutions were found which, although we did not prove uniqueness, are compatible with our numerical simulations and also a rigorous result for the maximum TSP in two dimensions. The solution of Eq. (93) was carried out by trying out different heuristics to construct the optimal path; it is possible that in more complex situations the method used here could serve as a useful indicator for such constructions.

Finally the idea of treating quenched variables as effectively annealed variables and then adjusting their Boltzmann weight in order to recover self-consistently the original quenched distribution may prove useful, either as an exact or approximate method in other problems involving quenched disorder. Indeed Morita's [18] pioneering work used this idea in an approximate context; here, we have shown that the procedure can be carried out exactly for this type of permutation based combinatorial optimization problem, as is also the case for some one-dimensional spin models [19].

ACKNOWLEDGMENTS

We would like to thank N. Read for drawing our attention to Ref. [20]. This research was supported in part by the National Science Foundation under Grant No. PHY99-07949.

[1] S. Kirkpatrick, C. D. Gelatt, Jr., and M. P. Vecchi, Science **220**, 671 (1983).
[2] O. C. Martin, R. Monasson, and R. Zecchina, Theor. Comput. Sci. **265**, 3 (2001).
[3] M. Mézard, G. Parisi, and M. A. Virasoro, *Spin Glass Theory and Beyond* (World Scientific, Singapore, 1987).
[4] Y. Fu and P. W. Anderson, J. Phys. A **19**, 1605 (1986).
[5] M. Mézard and G. Parisi, J. Phys. (Paris) **48**, 1451 (1987).
[6] J. Beardwood, J. H. Halton, and J. M. Hammersley, Proc. Cambridge Philos. Soc. **55**, 299 (1959).
[7] J. Vannimenus and M. Mézard, J. Phys. (France) Lett. **45**, L1145 (1984).
[8] M. Mézard and G. Parisi, Europhys. Lett. **2**, 913 (1986).
[9] W. Krauth and M. Mézard, Europhys. Lett. **8**, 213 (1989).
[10] A. G. Percus and O. C. Martin, Phys. Rev. Lett. **76**, 1188 (1996).
[11] A. G. Percus and O. C. Martin, J. Stat. Phys. **94**, 739 (1999).
[12] A. Barvinok, E. Kh. Gimadi, and A. I. Serdyukov, in *The Traveling Salesman Problem and its Variations*, edited by G. Gutin and A. P. Punnen, Combinatorial Optimization Series (Kluwer, Boston, 2002).
[13] P. E. Rouse, J. Chem. Phys. **21**, 1272 (1953).
[14] V. Desoutter and N. Destainville, Eur. Phys. J. B **37**, 383 (2004).
[15] D. E. Knuth, *Sorting and Searching*, 2nd ed., The Art of Computer Programming, Vol. 3 (Adison-Wesley, Reading, MA, 1988).
[16] D. Lancaster, J. Phys. A **37**, 1125 (2004).
[17] D. S. Dean, D. Lancaster, and S. N. Majumdar, cond-mat/0411111, J. Stat. Mech., L01001 (2005).
[18] T. Morita, J. Math. Phys. **5**, 1401 (1964).
[19] R. Kühn, Z. Phys. B: Condens. Matter **100**, 231 (1996).
[20] M. E. Dyer, A. M. Frieze, and C. J. H. McDiarmid, Oper. Res. Lett. **33**, 267 (1984).
[21] B. Derrida and O. Golinelli, Phys. Rev. A **41**, 4160 (1990).